AGU PUBLICATIONS

Geophysical Research Letters

RESEARCH LETTER

10.1002/2014GL061317

Key Points:
- The freezing ability of mineral dusts correlated with the K-feldspar content
- Among feldspars, microcline shows a better ice nucleation ability than orthoclase
- After coating, all investigated dusts feature a similar ice nucleation ability

Supporting Information:
- Text S1
- Text S2
- Table S1
- Table S2
- Table S3
- Readme
- Figure S1
- Figure S2

Correspondence to:
S. Augustin-Bauditz,
augustin@tropos.de

Citation:
Augustin-Bauditz, S., H. Wex, S. Kanter, M. Ebert, D. Niedermeier, F. Stolz, A. Prager, and F. Stratmann (2014), The immersion mode ice nucleation behavior of mineral dusts: A comparison of different pure and surface modified dusts, *Geophys. Res. Lett.*, *41*, 7375–7382, doi:10.1002/2014GL061317.

Received 24 JUL 2014
Accepted 23 SEP 2014
Accepted article online 26 SEP 2014
Published online 16 OCT 2014

The immersion mode ice nucleation behavior of mineral dusts: A comparison of different pure and surface modified dusts

S. Augustin-Bauditz[1], H. Wex[1], S. Kanter[1], M. Ebert[2], D. Niedermeier[1,3], F. Stolz[1,4], A. Prager[4], and F. Stratmann[1]

[1]Leibniz Institute of Tropospheric Research, Leipzig, Germany, [2]Institute of Applied Geosciences, Darmstadt, Germany, [3]Department of Physics, Michigan Technological University, Houghton, Michigan, USA, [4]Leibniz Institute of Surface Modification, Leipzig, Germany

Abstract In this study we present results from immersion freezing experiments with size-segregated mineral dust particles. Besides two already existing data sets for Arizona Test Dust (ATD), and Fluka kaolinite, we show two new data sets for illite-NX, which consists mainly of illite, a clay mineral, and feldspar, a common crustal material. The experiments were carried out with the Leipzig Aerosol Cloud Interaction Simulator. After comparing the different dust samples, it became obvious that the freezing ability was positively correlated with the K-feldspar content. Furthermore, a comparison of the composition of the ATD, illite-NX, and feldspar samples suggests that within the K-feldspars, microcline is more ice nucleation active than orthoclase. A coating with sulfuric acid leads to a decrease in the ice nucleation ability of all mineral dusts, with the effect being more pronounced for the feldspar sample.

1. Introduction

Ice particles influence both the cloud radiative properties and the cloud lifetime [*Storelvmo et al.*, 2011; *Lohmann and Diehl*, 2006]. Although ice nucleation research has been ongoing for many decades now, there are still many open questions concerning the formation of ice in clouds [e.g., *Hoose and Möhler*, 2012; *Murray et al.*, 2012]. There are two primary processes that can initiate ice nucleation in the atmosphere, homogeneous and heterogeneous ice nucleation [*Pruppacher and Klett*, 1997]. In contrast to the homogeneous ice nucleation, the heterogeneous ice nucleation is induced by a so-called ice nucleating particle (INP). This INP lowers the energy barrier for the phase transition from water to ice, causing ice nucleation at higher temperatures than observed for homogeneous ice nucleation (−38°C), for which no INP is present. Four different modes of heterogeneous ice nucleation are mentioned in the literature: deposition nucleation, immersion freezing, condensation freezing, and contact freezing [*Pruppacher and Klett*, 1997]. *Ansmann et al.* [2009] suggested the immersion freezing mode to be the most important freezing mode in mixed phase clouds, as they observed altocumulus clouds to almost always show a liquid cloud top before an onset of freezing was observed.

There are some criteria which determine if a particle can act as an INP or not [*Pruppacher and Klett*, 1997]. These criteria range from size (the bigger, the better) over lattice match and hydrogen bonds to cracks and defects on the surface of the particle. An early study from *Weickmann* [1951] already suggested that similarities between the lattice structure of a particle and an ice crystal could be responsible for the ice nucleation ability of some substances as, e.g., silver iodide. *Pruppacher and Klett* [1997], summarizing older studies, mentioned that clay particles were typically found in the central portion of snow crystals, and they discussed that the ice nucleation ability of, e.g., kaolinite, a clay mineral, might be derived from the close fit of its lattice structure to that of ice. For kaolinite, it was also stated, based on Monte Carlo simulations, that it is very likely that water molecules tend to be adsorbed in trench-like defects, facilitating the freezing process [*Croteau et al.*, 2010]. To date, there is still very little fundamental physical understanding about the surface structures that make a particle act as an INP.

In the past years, a significant part of the laboratory research on ice nucleation has focused on mineral dust (see reviews by *Murray et al.* [2012] and *Hoose and Möhler* [2012]) as these particles are known to be the most abundant INP in the atmosphere. Clay minerals comprise approximately two thirds of the total atmospheric dust mass [see *Atkinson et al.*, 2013, and references therein] and among these clay minerals, illite is the most abundant component [*Broadley et al.*, 2012].

crystal structure symmetries

monoclinic	$a \neq b \neq c$ $\alpha = \beta = 90°$ $\gamma \neq 90$	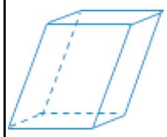
triclinic	$a \neq b \neq c$ $\alpha \neq \beta \neq \gamma \neq 90°$	

mineral group	endmember	structure symmetry
K-feldspar	microcline	triclinic
K-feldspar	orthoclase	monoclinic
Na-feldspar	albite	triclinic
Ca-feldspar	anorthite	triclinic

Figure 1. (top) Structure symmetry of crystals [*Vainshtein*, 1994]. (bottom) Exemplary overview listing some members of the feldspar group. There are additionally, different mixtures exists, where, e.g., a mixture between albite and anorthite is called plagioclase. Sanidine is a mixture containing K as well as Na feldspar and has a monoclinic crystal structure.

Recently, *Atkinson et al.* [2013] investigated the ice nucleation ability of K-feldspar, a mineral dust very common in the earth crust, with a cold stage cell. They found that freezing was already initiated at temperatures above −20°C. Additionally, they suggested that the ice nucleation of natural dust in general is controlled by the amount of K-feldspar in the aerosol particles. This idea was corroborated by *Wex et al.* [2014], who found that the ice nucleation ability of two kaolinite samples correlated with the amount of K-feldspar in them. *Yakobi-Hancock et al.* [2013] examined deposition ice nucleation of Arizona Test Dust (ATD), a chemically very heterogeneous substance, and its mineral components which include orthoclase, an end-member of the K-feldspar group. They found that the ice nucleation ability of orthoclase was similar to that of ATD, while other constituents showed a lower ice nucleation activity.

In our study, we show a comparison of the immersion freezing behavior of size-segregated mineral dust particles. New results of the immersion freezing ability of illite-NX and feldspar are presented and compared to existing data on ATD [*Niedermeier et al.*, 2011] and Fluka kaolinite [*Wex et al.*, 2014]. Experiments were carried out with the Leipzig Aerosol Cloud Interaction Simulator (LACIS) [*Hartmann et al.*, 2011]. Additionally, we show immersion freezing measurements with sulfuric acid coated mineral dust particles.

2. Materials and Methods

The illite-NX sample used in the present study was obtained from Arginotec (B + M Nottenkämper). The feldspar sample was provided by the Technical University Darmstadt and originated from Minas Gerais, Brazil. Both substances were examined in the framework of the Ice Nucleation research UnIT (INUIT) project.

The lattice structure of different minerals, e.g., illite and feldspar, is described in detail in *Murray et al.* [2012]. While clays generally have a layered structure, feldspars are composed of a lattice of tetrahedrals. The feldspar group contains a number of different end-members of which a few are given in Figure 1. The end-members differ from each other by the contained cations (K, Na, or Ca) and/or by their lattice structure symmetry (Figure 1).

The illite-NX investigated here contained mainly illite. Besides that, it contained some amounts of other materials such as quartz, kaolinite, and feldspar [*Atkinson et al.*, 2013]. The values given for the fractions of these individual materials contained in illite-NX differ in the data sheet provided by the manufacturer, and in the literature [*Broadley et al.*, 2012; *Möhler et al.*, 2008]. From our XRD analysis (X-ray diffraction, Panalytical X'Pert Pro, Almelo, Netherlands, equipped with a Cu X-ray tube and an automatic divergence aperture), we obtained a composition for illite-NX as shown in Table S1 in the supporting information. Furthermore, the XRD analysis revealed that the feldspars included in illite-NX (14% by mass) are most likely orthoclase (K-feldspar) and sanidine (Na and K-feldspar), but not microcline (K-feldspar). Unfortunately, it was not possible to quantify the exact amounts of these two feldspars. *Atkinson et al.* [2013] found that the amount of K-feldspar in illite-NX is 8%. It should be mentioned that the mass fractions of the different minerals and

particular the different feldspars contained in our samples are prone to uncertainties. However, combining the above listed information regarding the feldspar content in illite-NX, we assume that the illite-NX used in this study contains roughly 5% to 10% orthoclase. The feldspar sample used in our study consisted of 76% microcline (K-feldspar) and 24% albite (Na feldspar, see also Table S1 in the supporting information).

For the immersion freezing experiments presented here, size-segregated particles were used. Both pure and sulfuric acid coated particles were considered. The dry particle dispersion and the procedures for particle selection and coating closely follow those used during previous mineral dust related experiments with LACIS [*Niedermeier et al.*, 2010]. For dry generation of airborne dust particles, we used a fluidized bed generator (TSI 3400A, TSI Inc., St. Paul, Minnesota, USA). The sulfuric acid coatings were applied by means of a vapor diffusion tube, heated to temperatures of 70°C and 80°C. Downstream of the vapor diffusion tubes, the aerosol is passed over a water bath to increase the reactivity of the sulfuric acid with the particle surface [*Niedermeier et al.*, 2011]. Subsequent to charging the particles with a bipolar diffusion charger (Krypton 85), particles were size selected, adjusting for a mobility diameter of 300 nm. Thereto, a Differential Mobility Analyzer (DMA) [*Knutson and Whitby*, 1975], type Vienna Medium was used. Care was taken to minimize doubly charged particles by using a Micro-Orifice Uniform-Deposit Impactor (MOUDI, Model 100R, MSP Corporation) and a cyclone prior to the bipolar diffusion charger. Together these two devices provide a cut off diameter of 500 nm. However, due to bounce off effects, a certain number of doubly charged particles were still present and corrected for. This correction was based on the particle size distribution measured downstream of the DMA by means of an Ultra-High Sensitivity Aerosol Spectrometer, Droplet Measurement Technologies. A dilution system was used to adjust the particle number concentration. Subsequent to dilution, the aerosol flow was split into three streams. One stream was fed into a Condensation Particle Counter (TSI 3010) to measure the total particle number concentration. The other flow was fed into a Cloud Condensation Nucleus counter (CCNc) [*Roberts and Nenes*, 2005], Droplet Measurement Technologies to characterize the coating thickness (similarly done to, e.g., *Sullivan et al.* [2010] *Wex et al.* [2014]). The third flow was provided to LACIS. In the inlet section of LACIS, the aerosol flow is combined isokinetically with a humidified sheath air flow such that the aerosol forms a beam of approximately 2 mm in diameter along the center line of the flow tube. Supersaturated conditions were achieved by cooling the tube walls, and resulted in activation of the particles to droplets, with each droplet containing one size-segregated particle. These droplets then froze due to further cooling. For detailed information about the operation mode of LACIS see *Hartmann et al.* [2011].

At the outlet of LACIS, TOPS-Ice (thermally stabilized optical particles spectrometer) [*Clauss et al.*, 2013] was used to discriminate between frozen and unfrozen droplets and to quantify the frozen droplet fraction (f_{ice}, number of frozen droplets divided by the total number of frozen and unfrozen droplets). In the investigations presented here, f_{ice} was determined in the temperature range between −23°C and −40°C.

In this study, we also show results for ATD (Ultrafine Test Dust, Powder Technology Inc.) [*Niedermeier et al.*, 2011] and kaolinite (Fluka, Sigma Aldrich) [*Wex et al.*, 2014], which were also investigated with the above described measurement setup. The composition of these two materials is also given in Table S1 in the supporting information. The Fluka kaolinite related data shown here are slightly different to that from *Wex et al.* [2014], as here an additional multiple charge correction was applied to the data (see above). For the ATD data from *Niedermeier et al.* [2011] no multiple charged particles were detected.

3. Results

3.1. Intercomparison of Different Mineral Dusts and Their K-Feldspar Content

Figure 2 shows the results of the immersion freezing experiments for illite-NX (black) and feldspar (red). Additionally, data from previous LACIS studies concerning ATD (dark yellow) and Fluka kaolinite (blue) are shown. Since measurement setup and procedure, as well as the particle sizes (300 nm) were the same for all of the considered data, a direct quantitative comparison of f_{ice} measured for the different materials is possible. Large differences can be seen in f_{ice} for the different minerals. For the feldspar sample we detected ice already at approximately −23°C, whereas ATD, Fluka kaolinite and illite-NX particles nucleated ice in a detectable amount only at significantly lower temperatures (< -28°C). When looking at the corresponding K-feldspar contents of the different minerals one notices that the ice nucleation ability roughly scales with the K-feldspar content of the samples. This is in line with the results from *Atkinson et al.* [2013] who

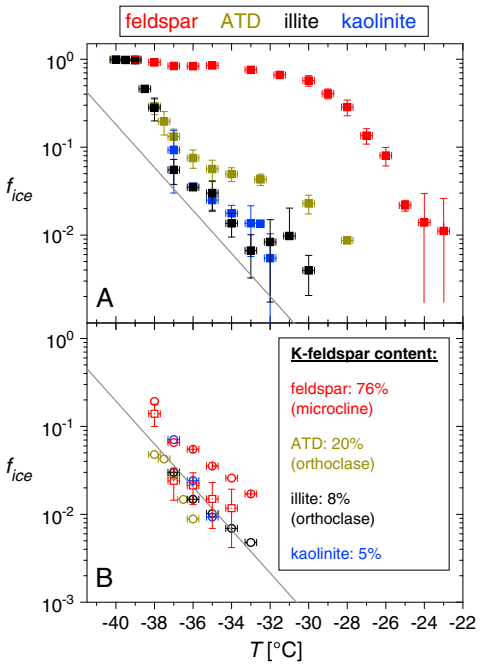

Figure 2. Measured ice fractions of feldspar (red) and illite-NX (black) as a function of temperature. Additionally, data from ATD (dark yellow) and Fluka kaolinite (blue) are shown. (a) Uncoated particles and (b) particles coated with sulfuric acid (circles: coating at 70°C; squares: coating at 80°C). Error bars are the standard deviation of the experiments and were obtained for temperatures with at least three measurements. For temperatures with fewer than three measurements, Poisson uncertainties are given. The gray line in both panels represents a fit curve through all the coated minerals (except the feldspar coated at 70°C) following the fit equation $f_{ice} = 3E - 11 \cdot e^{-0.563 \cdot T}$.

suggested that the K-feldspar content controls the freezing behavior of mineral dust particles. We will come back to this later in this chapter.

For the feldspar particles, f_{ice} reaches a plateau value of about 0.8 in the temperature range between −31°C and −38°C. Larger f_{ice} values are only observed at $T < -39$°C, i.e., at the temperature where homogeneous ice nucleation is the dominating ice nucleation mechanism. If we now assume that ice nucleation is induced at specific locations on the particle surface which are favorable for ice formation, i.e., at ice nucleation active (INA) sites, f_{ice} featuring a plateau with values below 1 implies that not all of the immersed 300 nm feldspar particles contained one or more of these INA sites [*Hartmann et al.*, 2013]. Applying a Poisson distribution to the INA sites over the particle population, we can determine an average number of INA sites per particle [*Hartmann et al.*, 2013]. For the 300 nm sized particles investigated here, this average number was found to be 1.8.

In Figure 3 we show the surface site densities (n_s) resulting from our measurements. n_s is often used to compare data from different studies. However, it should be mentioned that n_s depends on the actual particle surface area used for its determination, and neglects the time dependence of the freezing process [*Murray et al.*, 2012, and references therein]. For the data discussed here, determination of the particle surface area (mobility diameter was used) and nucleation time (approximately 1.6 s) were identical, so usage of n_s is straight forward and convenient. However, comparison of different experiments is more challenging as described in the supporting information. There we show that if particle surface area and ice nucleation time-related issues are treated correctly, our data and those of *Atkinson et al.* [2013] and *Broadley et al.* [2012] are in good agreement. In the supporting information we show equations for n_s, as well as for the nucleation rate coefficient j_{het}.

In the following we compare n_s values for the investigated mineral dust particles in relation to their K-feldspar contents. For that, best fit functions were calculated for the n_s values of illite-NX and feldspar in the temperature range where n_s shows a logarithmically linear increase with temperature. We are only using the respective data, because outside of the linear range, measurements are affected by droplet depletion (low temperatures, high n_s) and the lower f_{ice} detection limit (high temperatures, low n_s). The best fit functions are shown as black and red lines in Figure 3, respectively (the fit equations are given in the caption of Figure 3).

All the minerals investigated here contain certain amounts of K-feldspar, i.e., 76 %, 20 %, 5–10%, and 5 % by mass for our feldspar sample, ATD, illite-NX and kaolinite, respectively. As already mentioned, *Atkinson et al.* [2013] suggested that the K-feldspar component controls the ice nucleation ability of mineral dusts. Consequently, assuming that the n_s of the different samples scale with the mass fraction of K-feldspar seems a reasonable assumption. Under this assumption, the n_s for illite-NX should be roughly a factor of 10 lower (dotted red line in Figure 3) than that for our feldspar. Comparing the measured n_s-values of illite-NX (black symbols) to the scaled n_s fit (dotted red line) it becomes obvious, that scaling by a factor of 1/10 does not reproduce the measured n_s values at all. In fact, a reduction by a factor of roughly 1000 (dashed red line) is required to achieve somewhat comparable values. We did the same comparison between feldspar and ATD,

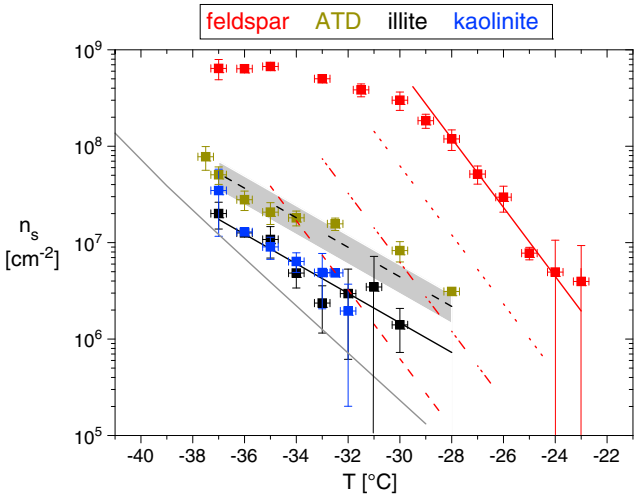

Figure 3. n_s values for the feldspar sample (red) and illite-NX (black) as a function of temperature. The straight lines are exponential fits to our data ($n_s = 0.0155 \cdot e^{-0.824 \cdot T}$ for feldspar and $n_s = 37.066 \cdot e^{-0.353 \cdot T}$ for illite-NX). The dotted, the dash-dotted and the dashed red lines represent the n_s fits of feldspar lowered by a factor of 10, 100 and 1000, respectively. The gray shaded area shows the n_s-fit of illite-NX increased by a factor of 2 to 4. The black dashed line is the n_s of illite-NX increased by a factor of 3, which corresponds to a K-feldspar mass fraction of 8%, as given in *Atkinson et al.* [2013]. The gray line represents the baseline which we assume to represent clay minerals, without any K-feldspar. The fit equation of the gray line is $n_s = 0.0029 \cdot e^{-0.606 \cdot T}$.

where the K-feldspar mass fraction in the feldspar sample is a factor of 4 above that in ATD. Instead, a factor of 100 is needed. From this we conclude that the differences in n_s cannot be explained by the different mass fractions of K-feldspar in the samples only. Furthermore, the dependence of n_s on temperature is different for the investigated minerals, which is indicative for the ice active sites not being identical with respect to their ice nucleation related properties (i.e., contact angle).

One could speculate that the observed behavior is due to the difference in the surface and bulk composition of the investigated particles. In other words the K-feldspar is not accessible at the surface, e.g., due to weathering. However, the different temperature dependencies and the fact that the illite-NX particles are the product of a purely mechanical deagglomeration process, make this explanation very unlikely.

As mentioned above, the K-feldspar contained in illite-NX and in ATD is likely orthoclase, while our feldspar sample contained mainly microcline. Indeed for ATD and illite-NX, n_s scales reasonably well with the mass fraction of orthoclase (20% and 5 to 10%, respectively). An increase of the n_s fit of illite-NX by a factor of 2 to 4 represents the ATD data quite well (gray shaded area in Figure 3). For Fluka kaolinite, it was not possible to identify if it is microcline or orthoclase which is present in the sample. Hence, we were not able to perform a similar comparison with Fluka kaolinite data.

In summary, the above described results suggest that among the K-feldspar group, the end-member microcline features a better ice nucleation activity than orthoclase. Indeed, already *Zimmermann et al.* [2008] found that microcline was the most ice active mineral dust in deposition ice nucleation, compared to, e.g., illite, kaolinite but also to albite (Na feldspar). So when trying to quantify heterogeneous ice nucleation induced by mineral dust, it is not only important to know the amount of K-feldspar, but it may also be essential to know which K-feldspar is actually present.

It is worth mentioning that both microcline and orthoclase feature the same molecular formula ($KAlSi_3O_8$) but are different with respect to their crystal structure symmetry. While microcline has a triclinic symmetry, orthoclase is monoclinic (see Figure 1). Hence, this difference in crystal structure symmetry might be the reason for the different ice nucleation abilities of the two K-feldspars. Nevertheless, it should be mentioned explicitly that a good ice nucleation ability is not necessarily connected to a triclinic crystal system, as, e.g., all Na feldspars and Ca feldspars are clearly less ice active than microcline [see *Atkinson et al.*, 2013]. It might be a combination of the crystal structure symmetry together with the present type of cation and the length of the different crystal axis which determine the ice nucleation activity of a mineral.

3.2. Effect of Sulfuric Acid Coating on the Ice Nucleation Ability of Mineral Dusts

We coated the mineral dust particles with sulfuric acid and explored whether and how chemical reactions between the acid and the particle material may change the ice nucleation ability of the mineral dusts. Droplet activation measurements with a CCNc were used to determine the thickness of the sulfuric acid coating on the particles. For coating temperatures of 70°C and 80°C, we found mean values of 3 and 15 nm effective coating thickness, respectively, independent of the mineral dust. In Figure S2 in the supporting information, an electron microscope picture of the feldspar particles coated at 80°C is shown as an example.

A sulfuric acid halo can be seen around the particles, indicating that the particles were completely coated. It should be noted that the droplets which are activated in LACIS grow to sizes of 3 µm and above, so that the coatings will form very dilute solutions around the insoluble dust particles (we calculated a water activity a_w of 0.9998 and 0.9994 for coatings done at 70°C and 80°C, respectively). Therefore, even in the case of the coated particles, a freezing point depression due to the dissolved sulfuric acid can be neglected.

In Figure 2 (bottom), the results of the immersion freezing experiments with the coated illite-NX and feldspar particles are shown as open symbols. Additionally, data for coated ATD and Fluka kaolinite are given. These particles were coated using the same method as presented here [*Niedermeier et al.*, 2010; *Wex et al.*, 2014]. Upon coating, all minerals showed a reduced ice nucleation ability compared to the uncoated particles. However, the decrease is strongest for the feldspar particles.

In the past it was found that the reduction in f_{ice} for coated ATD particles did not increase when the coating temperature was increased from 70°C to 85°C [*Reitz et al.*, 2011]. For our feldspar sample we observed a further smaller reduction in the ice nucleation ability when increasing the coating temperature from 70°C (open circles) to 80°C (open squares, Figure 2). It is likely that more sulfuric acid is required in order to destroy all the ice activity related to feldspar than for the other mineral dusts we present here. We assume that all ice activity related to feldspar were suppressed at 80°C, as the remaining ice activity became similar to that of the other coated mineral dusts.

It is well known that K-feldspar is converted to illite or kaolinite by weathering in nature, or, more generally, that weathering feldspars form clay minerals [*Meunier*, 2005; *Blum*, 1994; *Zhu et al.*, 2006]. During this process, which is called hydrolysis, K, Na, and Ca are released. Indeed, first results from X-ray photoelectron spectroscopy measurements (AXIS ULTRA, KRATOS Analytical Ltd., Manchester, UK, X-ray: monochromatic Al K 15 kV/10 mA), where we compared pure untreated feldspar with sulfuric acid treated feldspar showed that especially the amount of K is reduced after the treatment (Table S3). We assume that this leads to a change in the lattice structure, which may be the reason for the strong reduction in ice nucleation ability of K-feldspar.

For the ATD particles shown here (dark yellow symbols), *Niedermeier et al.* [2011] hypothesized that the clear decrease in the ice nucleation ability after coating ATD particles with sulfuric acid originated from aluminum silicates which were transformed to non ice active metal sulfates. In view of the results of the present study, an alternative interpretation would be that the K-feldspar (about 20 % orthoclase) contained in the ATD was affected. Similar conclusions could be made based on the Fluka kaolinite data. *Wex et al.* [2014] reported that particles from the Fluka kaolinite sample (blue symbols in Figure 2) which contained K-feldspar showed a reduced IN ability after coating with sulfuric acid, while another kaolinite sample which did not contain any feldspar (KGa-1b from the Clay Minerals Society), featured a low IN ability to begin with which was not affected by the coating. Our illite-NX data allow for the same conclusion. The orthoclase present in the illite-NX sample may have been chemically altered, which then leads to the slightly lowered ice nucleation ability of illite-NX.

Finally, when looking at the fully coated particles, it becomes obvious that all dusts fall together on a single line (gray curve in Figures 2a, 2b, and Figure 3, fit equations are given in the captions of both figures). This line may represent the ice nucleation ability of the "pure" clay minerals, i.e., the clay minerals without the feldspar. This implies that the ice nucleation behavior of the clay mineral proxies investigated is very similar and can be described/parameterized by a single fit equation. Nevertheless, it should be remembered, that the herein given n_s values were determined for geometric surface areas, i.e., based on mobility diameters and that the fit equation is only valid for LACIS nucleation times (1.6 s) and temperatures. In the supporting information, the influence of the ice residence time is examined in more detail.

4. Summary

In the present study the immersion freezing behavior of size-segregated illite-NX and feldspar particles was investigated as a function of temperature for both uncoated particles and particles coated with sulfuric acid. The measurements were carried out with LACIS, considering single, size-selected particles, immersed in highly diluted droplets. For illite-NX particles, freezing was observed in the temperature range below −30°C, implying that illite-NX has similar IN activity as the mineral dust particles previously examined with LACIS (ATD [*Niedermeier et al.*, 2011] and kaolinite [*Wex et al.*, 2014]). The feldspar particles, consisting mainly

of microcline, showed the best ice nucleation activity ever observed at LACIS for a mineral dust, with the initiation of freezing already at temperatures as high as −23°C.

When comparing the different dust samples it became obvious that the more K-feldspar is contained in the sample, the higher is the freezing ability. This is similar to what was found in *Wex et al.* [2014] for kaolinite and corroborates the findings of *Atkinson et al.* [2013], who suggested that the K-feldspar is responsible for the high ice nucleation ability of some mineral dusts. Furthermore, a comparison of the composition of ATD, illite-NX and feldspar led us to the hypothesis that within the K-feldspars, microcline is more ice nucleation active than orthoclase. Microcline and orthoclase differ only by their lattice structure, this could be interpreted as a hint that at least for K-feldspars the lattice structure influences the ice nucleation ability. This implies that when trying to quantify heterogeneous ice nucleation induced by mineral dust, it is not only important to know the amount of K-feldspar, it may also be necessary to know which K-feldspar is present in the sample.

Furthermore, we investigate how coating with sulfuric acid affects the ice nucleation ability of mineral dusts. For feldspar particles, we found a strong reduction of their ice nucleation ability. When considering sulfuric acid coated illite-NX (this study), Fluka kaolinite [*Wex et al.*, 2014] and ATD [*Niedermeier et al.*, 2011] particles, we found the decrease in ice nucleation ability of the respective mineral to be related to the K-feldspar content. This further corroborates that the ice nucleation behavior of mineral dusts may be controlled by the amount of K-feldspar being present. We also found that after coating with sufficient amounts of sulfuric acid, all investigated mineral dusts feature a similar ice nucleation ability. We hypothesize that the "remaining" ice nucleation ability is that of pure, feldspar free clay minerals, and that the ice nucleation ability is similar to all clay minerals.

What exactly is destroyed on the surface of the feldspar particles by the sulfuric acid coating could not be clarified completely within this study. It is also unclear if the sulfuric acid affected only the surface of the individual particles, or if the bulk chemical properties were altered. Further chemical and/or mineralogical analyses are necessary to clarify this completely. This could be key to answering the question: "What makes a particle an effective ice nucleating particle?".

Acknowledgments

This work is partly funded by the German Research Foundation (DFG projects WE 4722/1-1 and EB 383/3-1) within the DFG Research Unit FOR 1525 INUIT. We thank Rainer Petschick from the University of Frankfurt for doing the XRD measurements. D.N. acknowledges financial support from the Alexander von Humboldt Foundation. We would like to thank three anonymous reviewers for their comments and suggestions which improved the quality of the paper. Data can be made available upon request.

Geoffrey Tyndall thanks Hinrich Grothe, Zamin Kanji, and one anonymous reviewer for their assistance in evaluating this paper.

References

Ansmann, A., M. Tesche, P. Seifert, D. Althausen, R. Engelmann, J. Fruntke, U. Wandinger, I. Mattis, and D. Müller (2009), Evolution of the ice phase in tropical altocumulus: SAMUM lidar observations over Cape Verde, *J. Geophys. Res.*, *114*, D17208, doi:10.1029/ 2008JD011659.

Atkinson, J. D., B. J. Murray, M. T. Woodhouse, T. F. Whale, K. J. Baustian, K. S. Carslaw, S. Dobbie, D. O'Sullivan, and T. L. Malkin (2013), The importance of feldspar for ice nucleation by mineral dust in mixed-phase clouds, *Nature*, *498*, 355–358, doi:10.1038/nature12278.

Blum, A. E. (1994), Feldspars in weathering, in *Feldspars and Their Reactions*, edited by I. Parsons, pp. 595–630, Springer, Dordrecht, Netherlands.

Broadley, S. L., B. J. Murray, R. J. Herbert, J. D. Atkinson, S. Dobbie, T. L. Malkin, E. Condliffe, and L. Neve (2012), Immersion mode heterogeneous ice nucleation by an illite rich powder representative of atmospheric mineral dust, *Atmos. Chem. Phys.*, *12*, 287–307, doi:10.5194/acp-12-287-2012.

Clauss, T., A. Kiselev, S. Hartmann, S. Augustin, S. Pfeifer, D. Niedermeier, H. Wex, and F. Stratmann (2013), Application of linear polarized light for the discrimination of frozen and liquid droplets in ice nucleation experiments, *Atmos. Meas. Tech.*, *6*, 1041–1052, doi:10.5194/amt-6-1041-2013.

Croteau, T., A. K. Bertram, and G. N. Patey (2010), Observations of high density ferroelectric ordered water in kaolinite trenches using Monte Carlo simulations, *J. Phys. Chem. A*, *114*, 8396–8405, doi:10.1021/jp104643p.

Hartmann, S., D. Niedermeier, J. Voigtländer, T. Clauss, R. A. Shaw, H. Wex, A. Kiselev, and F. Stratmann (2011), Homogeneous and heterogeneous ice nucleation at LACIS: Operating principle and theoretical studies, *Atmos. chem. Phys.*, *11*, 1753–1767, doi:10.5194/acp-11-1753-2011.

Hartmann, S., S. Augustin, D. Niedermeier, J. Voigtländer, T. Clauss, H. Wex, and F. Stratmann (2013), Immersion freezing of ice nucleation active protein complexes, *Atmos. Chem. Phys.*, *13*, 5751–5766, doi:10.5194/acp-13-5751-2013.

Hoose, C., and O. Möhler (2012), Heterogeneous ice nucleation on atmospheric aerosols: A review of results from laboratory experiments, *Atmos. Chem. Phys.*, *12*, 9817–9854, doi:10.5194/acp-12-9817-2012.

Knutson, E. O., and K. T. Whitby (1975), Aerosol classification by electric mobility: Apparatus, theory and applications, *J. Aerosol Sci.*, *6*, 443–451, doi:10.1016/0021-8502(75)90060-9.

Lohmann, U., and K. Diehl (2006), Sensitivity studies of the importance of dust ice nuclei for the indirect aerosol effect on stratiform mixed-phase clouds, *J. Atmos. Sci.*, *63*, 968–982, doi:10.1175/JAS3662.1.

Meunier, A (2005), *Clays*, Springer, Berlin, Germany.

Möhler, O., S. Benz, H. Saathoff, M. Schnaiter, R. Wagner, J. Schneider, S. Walter, V. Ebert, and S. Wagner (2008), The effect of organic coating on the heterogeneous ice nucleation efficiency of mineral dust aerosols, *Environ. Res. Lett.*, *3*, 025007, doi:10.1088/1748-9326/3/2/025007.

Murray, B. J., D. O'Sullivan, J. D. Atkinson, and M. E. Webb (2012), Ice nucleation by particles immersed in supercooled cloud droplets, *Chem. Soc. Rev.*, *41*, 6519–6554, doi:10.1039/c2cs35200a.

Niedermeier, D., et al. (2010), Heterogeneous freezing of droplets with immersed mineral dust particles—Measurements and parameterization, *Atmos. Chem. Phys.*, *10*, 3601–3614, doi:10.5194/acp-10-3601-2010.

Niedermeier, D., et al. (2011), Experimental study of the role of physicochemical surface processing on the IN ability of mineral dust particles, *Atmos. Chem. Phys.*, *11*, 11,131–11,144, doi:10.5194/acp-11-11131-2011.

Pruppacher, H. R., and J. D. Klett (1997), *Microphysics of Clouds and Precipitation*, Kluwer Acad., Dordrecht, Netherlands.

Reitz, P., et al. (2011), Surface modification of mineral dust particles by sulphuric acid processing: Implications for ice nucleation abilities, *Atmos. Chem. Phys.*, *11*, 7839–7858, doi:10.5194/acp-11-7839-2011.

Roberts, G. C., and A. Nenes (2005), A continuous-flow streamwise thermal-gradient CCN chamber for atmospheric measurements, *Aerosol Sci. Technol.*, *39*(3), 206–221, doi:10.1080/027868290913988.

Storelvmo, T., C. Hoose, and P. Eriksson (2011), Global modeling of mixed phase clouds: The albedo and lifetime effects of aerosols, *J. Geophys. Res.*, *116*, D05207, doi:10.1029/2010JD014724.

Sullivan, R. C., et al. (2010), Irreversible loss of ice nucleation active sites in mineral dust particles caused by sulfuric acid condensation, *Atmos. Chem. Phys.*, *10*, 11,471–11,487, doi:10.5194/acp-10-11471-2010.

Vainshtein, B. K. (1994), *Fundamentals of Crystals: Symmetry, and Methods of Structural Crystallography (Modern Crystallography)*, vol. 1, Springer, Berlin, Germany.

Weickmann, H. K. (1951), A theory of the formation of ice crystals, *Arch. Meteorol. Geophys. Bioklimatol., Ser. A*, *4*(1), 309–323.

Wex, H., P. J. DeMott, Y. Tobo, S. Hartmann, M. Rösch, T. Clauss, L. Tomsche, D. Niedermeier, and F. Stratmann (2014), Kaolinite particles as ice nuclei: Learning from the use of different kaolinite samples and different coatings, *Atmos. Chem. Phys.*, *14*, 5529–5546, doi:10.5194/acp-14-5529-2014.

Yakobi-Hancock, J. D., L. A. Ladino, and J. P. D. Abbatt (2013), Feldspar minerals as efficient deposition ice nuclei, *Atmos. Chem. Phys.*, *13*, 11,175–11,185, doi:10.5194/acp-13-11175-2013.

Zhu, C., D. R. Veblen, A. E. Blum, and S. J. Chipera (2006), Naturally weathered feldspar surfaces in the Navajo Sandstone aquifer, Black Mesa, Arizona: Electron microscopic characterization, *Geochim. Cosmochim. Acta*, *70*, 4600–4616, doi:10.1016/j.gca.2006.07.013.

Zimmermann, F., S. Weinbruch, L. Schütz, H. Hofmann, M. Ebert, K. Kandler, and A. Worringen (2008), Ice nucleation properties of the most abundant mineral dust phases, *J. Geophys. Res.*, *113*, D23204, doi:10.1029/2008JD010655.